JOURNAL OF AIRCRAFT
Vol. 37, No. 5, September–October 2000

Near-Field Interaction of a Jet with Leading-Edge Vortices

Frank Y. Wang,* Michael M. J. Proot,† and Jean-Marc Charbonnier‡
von Kármán Institute for Fluid Dynamics, 1640 Sint-Genesius-Rode, Belgium
and
Pasquale M. Sforza§
University of Florida, Shalimar, Florida 32579

Results of the interaction between the vortex-wake of a 75-deg leading-edge sweep delta wing and a circular jet issuing from a tube parallel to the centerline of the wing are presented. Laser lightsheet flow visualizations and total pressure measurements were used to characterize the flowfield. In addition, a vortex-filament model used to supplement the examination of the streamwise evolution of jet exhaust in the presence of trailing vortices was shown to provide a reasonable qualitative description of the observed flow behavior. Visualization and total-pressure data revealed that introduction of large-scale persistent streamwise vortices substantially augments the jet spreading. Moreover, such an occurrence can be achieved within a short distance downstream.

Nomenclature

c	=	chord
d	=	jet orifice diameter
P_0	=	total pressure
q_∞	=	freestream dynamic pressure
r	=	jet orifice radius
t	=	time
V_∞	=	freestream velocity
W	=	downwash velocity
x	=	spanwise coordinate
y	=	normal coordinate
z	=	streamwise coordinate
α	=	angle of attack
Γ_j	=	circulation of vortices from jets
Γ_w	=	circulation of vortices from wing planforms
ε	=	wing apex half-angle

Introduction

THE interaction of vortices from aerodynamic planforms with a jet plume represents a subject of academic and practical interest as it spans many technological areas. In the context of developing a large second-generation supersonic transport fleet, it becomes important to determine whether ozone-depleting products from engine exhaust entrained in the vortex-wake experience conditions that are substantially different from what would otherwise have been envisioned, thereby affecting the initial dispersion and the photochemical processing of various species.[1–5] The exhaust effluent entrained in the vortex wake can have a very different residence time than what is usually expected, as the normal vertical transport of pollutants out of the stratosphere is quite slow.[6] A similar environmental concern exists for the present subsonic transport fleets, as the initial dispersion and entrainment characteristics of engine exhaust influence the formation of those products that may be considered pollutants.[7–11] Therefore, depending on the geometry and scale of the vortex-wake/plume interaction in the near field, different initial distribution and disposition of the contaminants could occur, possibly generating a significant impact on the ultimate design and operation of future commercial aircraft. This interaction can also alter the wake signature of military aircraft, thereby influencing target acquisition effectiveness of optically based sensors.[12] Furthermore, vortex-plume interaction modifies the acoustic and mixing characteristics of high-speed jets, which is of significant importance.[13–15] In recognition of the increasing importance of this subject and the scarcity of published experimental information on this interaction in any speed range, the present authors initiated an exploratory study to examine the fundamental aspects of the interaction at low speed, and the results to date[16,17] are summarized in this paper. An experimental investigation was launched consisting of lightsheet flow visualization at three planform angles-of-attack and at three downstream stations. For the median angle-of-attack case, the interaction was also characterized by total-pressure measurements along the jet centerline. The utility of a simple engineering model to provide additional insights on the experimental data and determine the downstream location at which significant mixing interaction should begin was also illustrated.

Experimental Setup

Although the development of an aircraft vortex wake can be divided into distinct phases such as roll up and viscous decay with possible breakup because of Crow instability, the present investigation focuses on the initial development of the jet in the near-field region. Motivated by achieving interaction rapidly within the wind-tunnel test-section length available, a sharp-edged delta wing that generates strong vortices was chosen as the planform. A delta wing also represents a planform of practical interest as it has been incorporated in many aircraft designs. The model was a sharp-edged 75-deg sweepback delta wing supported by a streamlined strut 5 mm in thickness. The span at the trailing edge of the delta wing was 76 mm. An unheated air jet was introduced via a 4 mm i.d. circular tube mounted under the wing and along the centerline with the exit at the trailing edge. The mass flow of the jet was monitored by a rotameter, from which the mean velocity of the jet at its exit was inferred. The freestream conditions were measured with a water manometer. The ratio of bulk velocity of the jet to freestream was fixed at 2 and 2.4 in the flow visualizations and pressure measurements, respectively, in the results presented here. This range of jet-to-freestream ratio was chosen as representative of the value for

Received 23 March 1999; revision received 9 December 1999; accepted for publication 10 December 1999. Copyright © 2000 by the American Institute of Aeronautics and Astronautics, Inc. All rights reserved.

*National Science Foundation-NATO Postdoctoral Fellow, Department of Aeronautics and Aerospace, Waterloose Steenweg 72; currently National Research Council Research Associate, Mail Stop 86-7, NASA John H. Glenn Research Center at Lewis Field, 21000 Brookpark Road, Cleveland, Ohio 44135. Senior Member AIAA.

†Diploma Course Member, Department of Aeronautics and Aerospace, Waterloose Steenweg 72; currently Research Staff, Delft University of Technology, Department of Aerospace Engineering, Kluyverweg 1, 2629 HS Delft, The Netherlands.

‡Associate Professor, Department of Aeronautics and Aerospace, Waterloose Steenweg 72; currently Centre National d'Etudes Spatiales/Toulouse Space Center, Mars Exploration Program, BPI 2222, 18 Avenue Edouard Belin, 31 401 Toulouse Cedex 4, France.

§Director and Professor, Graduate Engineering and Research Center, 1350 N. Poquito Road. Associate Fellow AIAA.

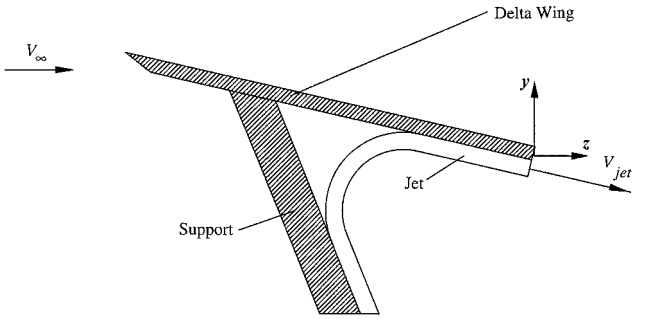

Fig. 1 Schematic side view of the wing-jet combination under consideration.

aircraft at cruise.[18] A schematic illustration of the wing-jet combination is shown in Fig. 1. The experiments were carried out in the VKI-L2A low-speed facility. It is an open circuit tunnel operating in the suction mode, with an axisymmetric 8:1 contraction faired to an octagonal test section 0.28 m in width and 1.30 m in length in which the maximum velocity is 45 m/s.

For the flow-visualization study the tunnel was operated at 10.0 ± 0.05 m/s, thereby yielding a jet Reynolds number of 5.5×10^3 based on orifice diameter. Two systems of seeding particles were used for the freestream and the jet. Freestream flow was seeded using particles on the order of 1μ diameter obtained by vaporizing fog oil droplets and introducing them through the inlet of the tunnel. The jet flow was seeded by enclosing burning incense in a pressurized vessel fed with an air supply line, which then forced the smoke through the simulated jet exhaust. The choice of this smoke generation method was based on its simplicity, its low susceptibility to condensation in a small tube, and its typically submicron range particulate diameter. A 7-W Ar-Ion laser with a cylindrical lens was used to produce a simple, uncollimated lightsheet at various distances downstream. Visualization was limited to a maximum distance of three chord lengths downstream because of space constraints around the tunnel area. Lightsheet visualizations with either the freestream or the jet seeded were made for an angle-of-attack range of 5 deg $\leq \alpha \leq$ 25 deg in 5-deg increments. The value of α at which vortex breakdown would occur for a 75-deg sweepback delta wing is approximately 33–35 deg, which was confirmed during the course of the experiments. The upper bound $\alpha = 25$ deg thus does not venture into a region where additional complexity is introduced by vortex breakdown.

For pressure probe measurements a 0.3-mm i.d. pitot probe connected to a 35-mm H_2O range Validyne^{TM} pressure transducer was used. To increase the sensitivity of the transducer during measurements, a higher, 32.0 ± 0.45 m/s, bulk velocity for the jet was used, making the Reynolds number of the jet 8.8×10^3 based on the orifice diameter. The total pressure investigation was limited to the center plane of the jet and one angle of attack, i.e., 15 deg.

Flow-Visualization Results

With only the freestream flow seeded and without introducing the jet plume, the visualized vortex wake of the delta wing exhibited the classical pattern for all angles examined. Of the various features present the most distinguishing were the two large black holes, representing the cores of the primary vortices, which are formed as a consequence of the seeding particles being centrifuged away. With the simulated jet exhaust activated, no discernible difference was visualized in the resulting vortex wake, concurring with the finding of Ref. 18. However, for the case where only the jet was seeded, a very remarkable spreading of the jet was observed for all angles of attack tested. The visualization photographs for the cases of $\alpha = 5$, 15, and 25 deg are shown in Fig. 2. In all cases the photographs were recorded from a vantage point behind the planform and looking upstream obliquely. A 35-mm camera fitted with a 50-mm lens and loaded with Kodak^{TM} TMAX ASA-3200 film was used. The exposure times used for these photographs were in the range of $\frac{1}{4}$–$\frac{1}{2}$ of a second. This range of exposure time was selected to obtain the

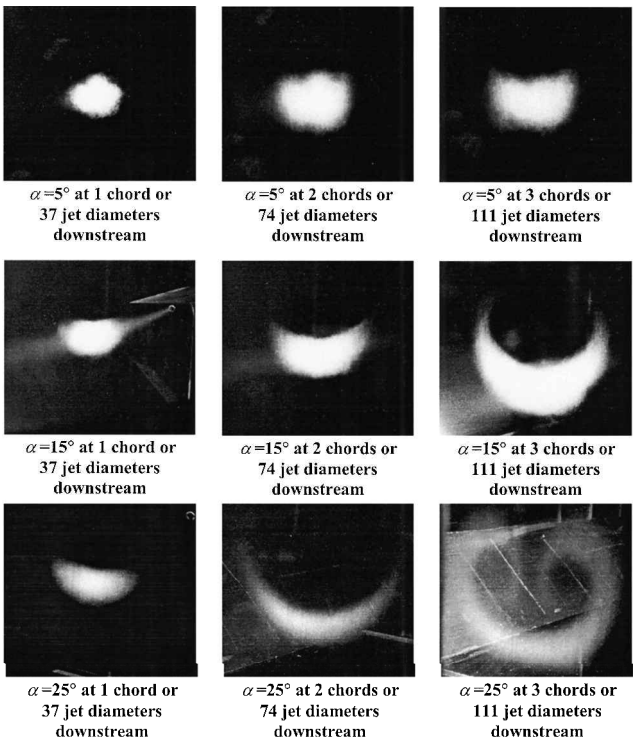

Fig. 2 $\alpha = 5, 15,$ and 25-deg flow visualization with the jet alone seeded.

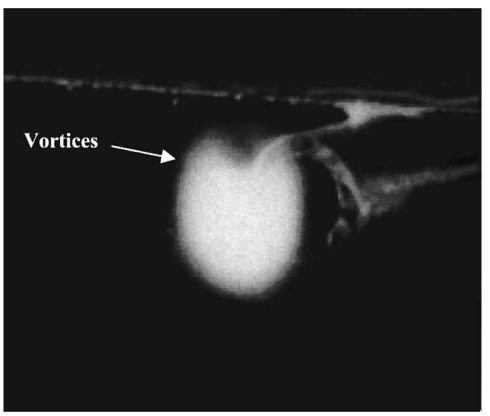

Fig. 3 α = 5 deg visualization performed at the jet plume exit. A counter-rotating vortex pair is developed, and the overall pattern resembles that of the crossflow over an inclined slender body.

time-averaged shape of the turbulent jet.

Overall, well-organized streamwise vortices of the planform can increase the jet spread rate considerably. Moreover, very large spanwise spreading can be achieved at moderate angles of attack and within a short distance of three root chords downstream. At $\alpha = 25$ deg and three chords away flow visualization revealed the onset of jet effluent being ingested into the wing vortices. Therefore for the current wing-jet combination the horizontal spreading of the jet would be restricted by the spacing between the wing vortices and achievable within three wing chords downstream. In addition, the development of streamwise vortices as the result of the jet exhausting into the planform vortex wake was evident. Using $\alpha = 5$ deg as an example, this particular point is illustrated in Fig. 3, where visualization was performed at the jet plume exit. A counter-rotating vortex pair is developed, and the overall pattern is that of the crossflow over an inclined slender body. The streamwise vortices developed around the jet stem from a resultant transverse flow relative to the jet exit. More specifically, the simulated jet, being aligned with the wing chord, would experience a crossflow resulting from the downwash of the planform as well as from being at an inclination to

the freestream flow. The $\alpha = 5$ deg flow visualization revealed that shape of the jet resembled a w up to two chords downstream and then evolved to the u shape at three chords away. At higher angles of attack, only the u shape was observed at the three stations examined. With the assistance of a simple analytical model whose details are to be presented later, these experimental observations can be explained in terms of vortex dynamics. In short, the w cross-sectional shape of the jet at $\alpha = 5$ deg is believed to have been caused by vortices generated by the jet being in close proximity to the jet centerline. As such, the vortices produced by the jet induce a velocity field near the jet and locally create the pronounced indentations near the center of the jet. A jet shape resembling a w is thus produced. As the jet vortices move further away from the centerline of the jet—a consequence of being under the induction influence from the stronger wing vortices, the jet cross section then merely evolved to resemble a u shape. Although the photographs shown in Fig. 2 are those representing integrated views over time, they are very similar to images of the jet taken at a camera shutter speed of $\frac{1}{500}$ of a second. For example, these shorter exposure photographs for the two and three chords downstream stations at $\alpha = 5$ deg are shown in Fig. 4, in which their respective w and u shapes are distinctly seen.

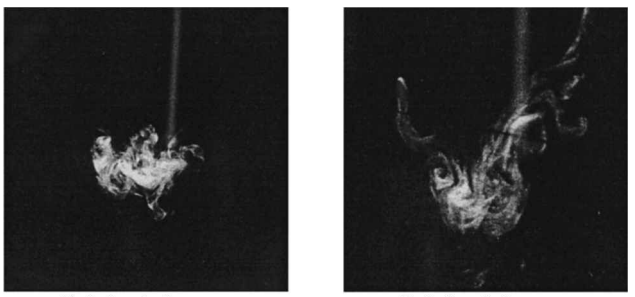

Fig. 4 Examples of the same α = 5 deg visualization with short exposure time.

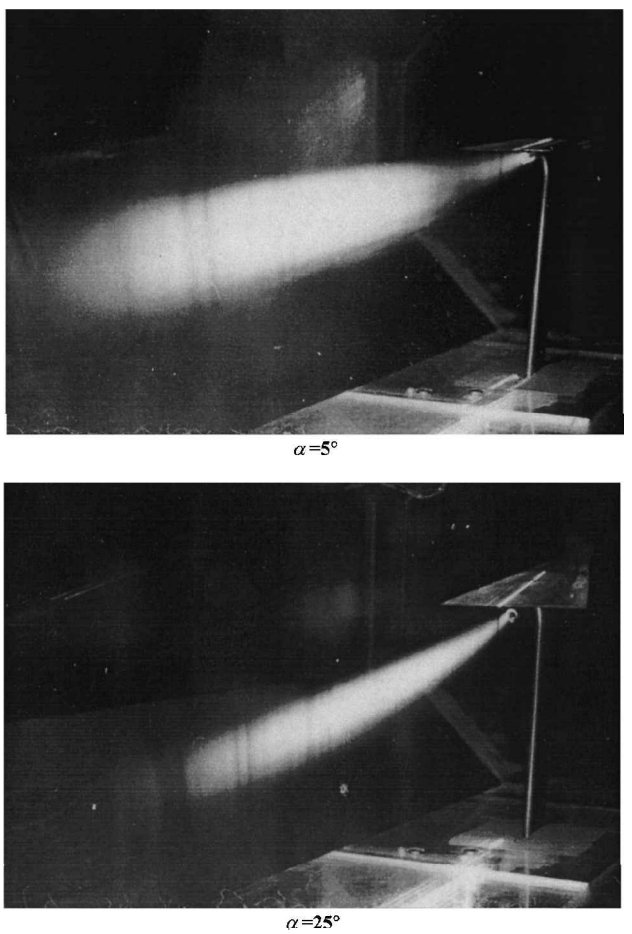

Fig. 5 Flow visualization along the jet centerline.

The crossflow plane lightsheet visualization also revealed a compression of the jet shape in the normal direction with increasing angle of attack. This phenomenon is again depicted in the lightsheet visualization taken along the centerline of the jet, as shown in Fig. 5 for the two extreme angles of attack cases.

Total-Pressure Survey Results

Total-pressure measurements were performed for the intermediate case of $\alpha = 15$ deg. These surveys were made at downstream distances of $z/d = 3.58$, 13.25, 22.7, and 33.13. The last survey location represents a downstream distance slightly less than one wing chord away. To account for any misalignment that may have existed in the experimental setup, surveys were first made vertically and horizontally to locate the maximum total pressure reading in the jet at each z/d location. After the maximum total-pressure location was found, vertical traverses were then made, in increments of 0.5 mm, for both jet-on and jet-off conditions. The difference between the total pressure at the surveyed location and that of the freestream is normalized with freestream dynamic pressure. The results of the total-pressure surveys are shown in Fig. 6, whose associated maximum uncertainty is 4.3% in the jet region. In each of the surveys performed with the jet activated, the registered total pressure in the vicinity of the upper jet boundary has a localized deficit whose magnitude gradually diminishes as the jet travels downstream. The wake flow from the trailing edge of the planform is believed to be responsible for this artifact. Likewise, some influence from the wake of model support is seen in the lower portion of the jet.

The velocity profiles may be inferred if the assumption is made that the static pressure is constant through the mixing region. Upon making this approximation, the nondimensional maximum excess velocity as a function of downstream distance is presented in Fig. 7. In constructing Fig. 7 from existing data, it was necessary to assume a velocity profile at the jet orifice. Two limiting cases were considered so as to cover a range of likely maximum velocity at the exit: a $\frac{1}{7}$th power law profile and a top-hat profile. First, a reduction in the potential core length is observed compared to its coaxial jet counterpart.[19] In addition, as vortex-augmented jet spreading occurs, an accompanying decrease in the maximum velocity of the jet would take place to conserve the momentum of the jet. The jet then decays at a faster rate for distances beyond 10 diameters downstream compared to a coflowing jet at the same jet-to-freestream velocity ratio. Also confirming the flow-visualization results, these measurements illustrate the descending trajectory of the jet.

Modeling of Jet/Vortex-Wake Interaction

To facilitate additional interpretations of the experimental findings and provide insights on the sensitivity of various parameters on aspects of the interaction, it is desirable to have a simple model. The development of such a model, its utility, and the interplay with the experimental artifacts are discussed in the following paragraphs.

The first component of the modeling is that of the vortex wake. In the absence of vortex breakdown, the evolution of the vortex wake in the near field can be described with inviscid vortex methods.[20,21] Suitable modeling of the jet can likewise be accounted for using vortex dynamics, and the rationales are as follows. As already stipulated, the jet exhausting into the vortex wake of the planform is immersed in a weak crossflow. The magnitude of the crossflow can be approximated by the expression

$$V_\infty \sin(\alpha) - W \cos(\alpha)$$

where W is the downwash generated by the planform.

As was illustrated by the visualization experiments, among the distinguishing characteristics of subsonic jets in subsonic crossflows is their development into a counter-rotating vortex pair that convects downstream with the coflow. Fearn and Weston[22] reported that these vortices are more persistent than other characteristics and

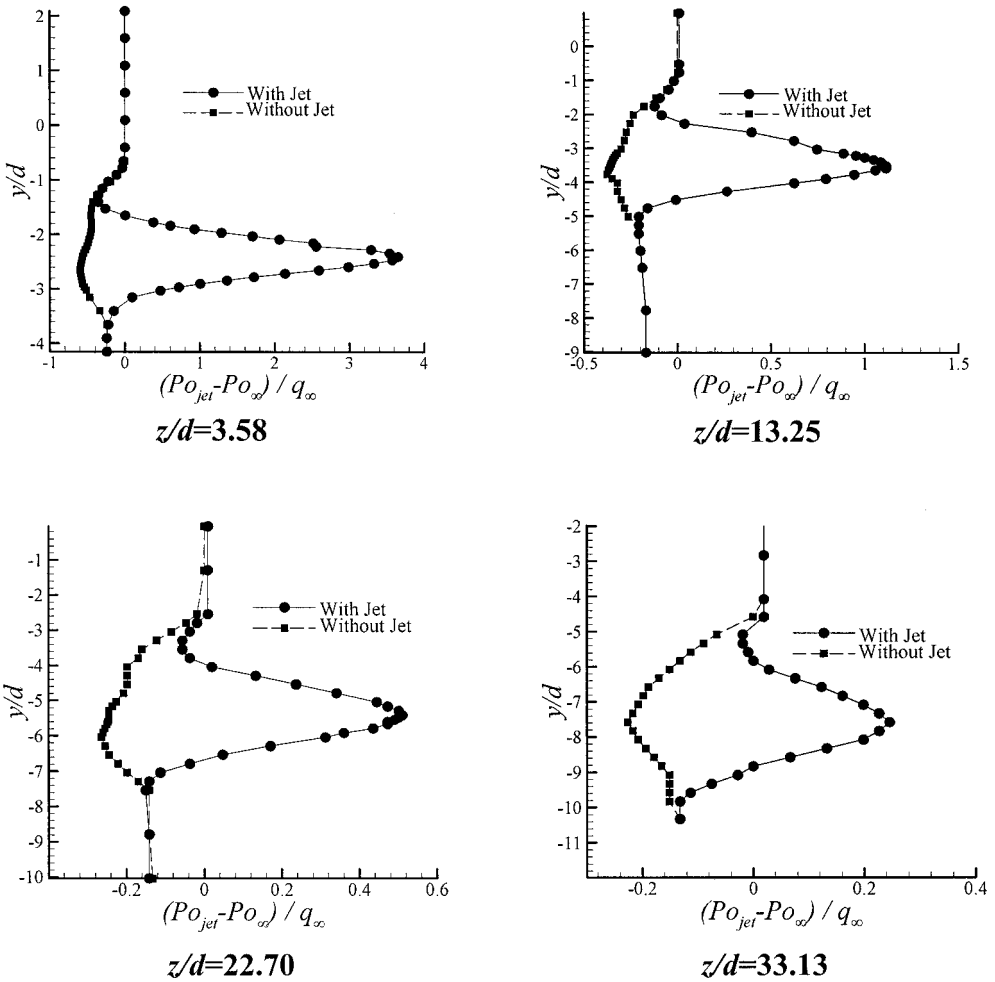

Fig. 6 Centerline total-pressure surveys of the jet for α = 15 deg.

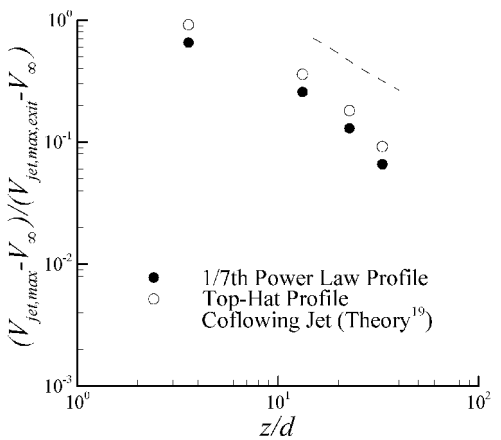

Fig. 7 Velocity decay of the jet exhausting into the α = 15 deg vortex wake vs that of a coflowing jet at the same freestream-to-jet-velocity ratio.

they dominate the flowfield for distances greater than about 10 diameters downstream of the jet orifice. The important parameter for such flows is the ratio of the jet velocity to the crossflow velocity. For small crossflows, as would be in the present case, the vortex development is strong. In light of the vortex-dominating features, development of the interacting wake flow at low speed could likewise be assessed with vortex-filament analysis, as was done by Sforza[23] for the case of supersonic interaction. The problem then reduces to the interaction between vortices generated by the planform and those of the jet. The interaction between the pairs of wing and jet vortices can then be investigated by following the spatial evolution of the vortices themselves and the induced flowfield around them by means of classical vortex-filament analysis. The necessary initial conditions to be prescribed would be the locations and the strengths of the wing and jet vortices. In this investigation location of the wing vortices at the trailing edge of the planform were taken from the experimental data of Kimball,[24] which were collected in the same wind tunnel. For the prescription of leading-edge vortex circulations, the following semi-empirical relation of Hemsch and Luckring[25] and Traub[26] is used:

$$\Gamma_w / V_\infty c = 4.63 \cdot \tan^{0.8}(\varepsilon) \cdot \tan^{1.2}(\alpha) \cdot \cos(\alpha) \qquad (1)$$

The lack of coherent information on the trajectory and circulation of vortices developed from jets in crossflows as encountered by Sforza[23] in modeling the supersonic interaction is also experienced in the present subsonic case. In the interest of making the modeling as consistent and self-contained as possible, the basic premise outlined in Sforza[23] is used; that is, consideration of the initial jet as a solid slender cylindrical body at incidence. Vortices are then developed from the resultant velocity component normal to this imaginary solid body. The associated circulations were prescribed so that their induced centerline velocity balances the resultant crossflow acting on the jet exit. For a jet positioned at the center of the trailing edge and aligned along the centerline chord, a configuration used in the flow-visualization experiment (Fig. 1), the circulation of the jet vortices in the present framework becomes

$$\Gamma_j = \pi(d/2)[V_\infty \sin(\alpha) - W\cos(\alpha)] \qquad (2)$$

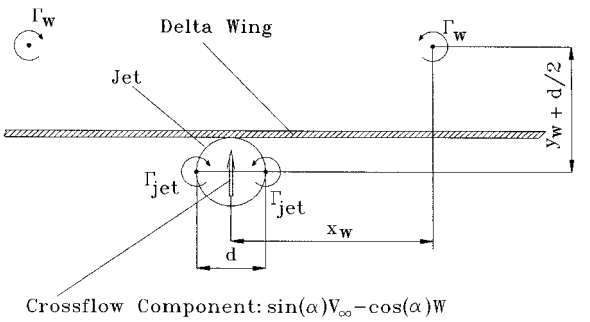

Fig. 8 Initial conditions for the vortex filament calculations. All vortex circulations are positive as shown.

The initial locations of the jet vortices in this particular formulation have been placed horizontally at one jet diameter apart with respect to the jet center. For the present calculations the origin is located on the trailing edge at the midspan of the delta wing, and therefore the circulation of the jet-induced vortices can be written as

$$\Gamma_j = \pi \frac{d}{2} V_\infty \sin(\alpha) \left\{ 1 - \frac{x\Gamma_w}{\pi[x^2 + (y + d/2)^2]} \right\} \tag{3}$$

where positive x and y are directions toward the wing starboard side and upward normal to the freestream, respectively. The initial conditions of the vortex filament calculations are illustrated in Fig. 8. All vortex circulations are positive as shown. The sign of the jet vortices, once indicated by the direction of the crossflow component, is then fixed and allowed to trail downstream. The proposed representation of the jet excludes the momentum effect of the exhaust. Additional considerations such as the entrainment characteristics of the jet and that of the leading-edge vortices, as well as the effect of buoyancy, are not considered at this time. As both wing and jet vortex systems roll up rapidly, modeling of the rolling-up process are also neglected.

The interaction between the pairs of wing and jet vortices in the near field is then investigated using the semi-infinite form of the Biot–Savart Law[27]:

$$\frac{dx}{dt}(x, y) = -\frac{1}{4\pi} \sum_{k=1}^{N} \frac{\Gamma_k (y - y_k)}{(x - x_k)^2 + (y - y_k)^2} \tag{4a}$$

$$\frac{dy}{dt}(x, y) = \frac{1}{4\pi} \sum_{k=1}^{N} \frac{\Gamma_k (x - x_k)}{(x - x_k)^2 + (y - y_k)^2} \tag{4b}$$

where dx/dt and dy/dt are the vortex-induced velocities of each location in a Lagrangian space and the subscript k denotes the individual vortices. The spatial evolution of the flowfield is then obtained by integrating Eq. (4) using the Adams–Bashford scheme, which is recommended for vortex methods[28]:

$$\boldsymbol{x}_j(t + \Delta t) = \boldsymbol{x}_j(t) + \Delta t \left[\tfrac{3}{2} u(\boldsymbol{x}_j, t) - \tfrac{1}{2} u(\boldsymbol{x}_j, t - \Delta t) \right] \tag{5}$$

To initiate the Adams–Bashford scheme, the first-order Euler method was used during the first time step to provide the necessary condition. The singular behavior of the vortex point method can be avoided by prescribing a vorticity distribution to represent the vortex cores. This, however, is not incorporated in the present study. The decay of the vortices, usually treated by introducing variable cores and circulations, is likewise neglected in the present paper.

Results of Calculations and Discussion

As dictated by the tunnel restrictions on the experiments, calculations were terminated at a time step corresponding to the same maximum distance of three chords downstream. Calculations were made in the angle-of-attack range of 2.5–30 deg. A particular dilemma faced in carrying out calculations was the characterization of the jet boundary in the computed results. It is proposed here that the trajectory of the jet vortices be used as a global description for jet development, even though it is recognized that the boundary of the jet would actually occupy a spatial extent larger than that suggested by the horizontal separation distance of the two jet vortices. To quantify the extent by which the jet has been influenced by the wing vortices, a parameter Ω, defined as the ratio of the horizontal distance between the jet vortex centers with and without the presence of the wing vortices, is introduced. This parameter provides an indication of the additional rate of strain on the jet induced by the mutual interaction of the various vortices. Figure 9 illustrates the variation of Ω with angle of attack and demonstrates the extent to which the introduction of organized and persistent wing vortices can increase the spreading of the jet. For example, at a short distance of only three chords away, a nearly 900% increase in jet spread is achieved for the planform at $\alpha = 15$ deg. The jet spreading behavior is even more pronounced at higher angles of attack. As the angle of attack increases, the strengths of the wing and jet vortices increase nonlinearly, and at the same time their initial distances with respect to each other increase. The calculations also revealed that, for the cases considered, wing vortices were only slightly drawn toward the jet center by the induced velocity field created by the jet vortices.

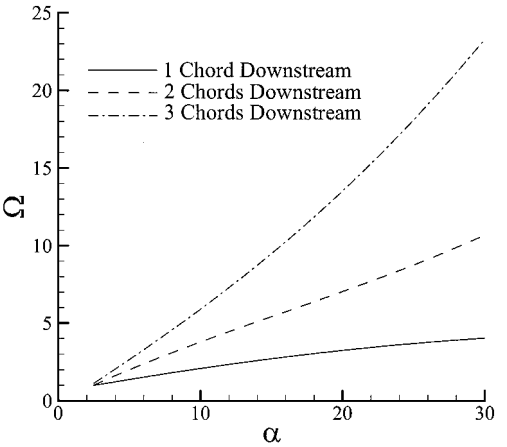

Fig. 9 Spreading characteristic of the jet vortices with angle of attack.

To further facilitate the interpretation of these calculations, a ring of tracer particles, modeled as vortices of zero circulation, was released from the perimeter of the jet, and its downstream evolution was followed. These results are presented in Fig. 10. Overall, comparisons between the flow-visualization photographs with their computed tracer particle patterns of Fig. 10 show good qualitative agreement. The $\alpha = 5$ deg results suggest that if the jet itself were seeded and a lightsheet visualization performed one would observe a jet that starts out as a circle, widens, and deforms to a shape resembling very much a w at one to two chords downstream and then continues to spread while deforming into a u-like shape three chords away. Similarly, the calculated $\alpha = 15$ and 25-deg cases reveal the distorted jet only has the u shape and increasingly elongates in the horizontal direction. These findings are consistent with the flow-visualization results presented earlier. Unfortunately, no provision was made to correct for the perspective distortion in the flow-visualization photographs so that the spread of the jet could have been compared quantitatively. Nevertheless, useful insights on the experimental observations have been obtained. Inferring from the calculated results, the cross-sectional shape of the jet observed experimentally in the $\alpha = 5$ deg case appears because of the vortices from the jet being in close proximity to the central part of the jet, creating the localized dents on the jet, which ultimately shaped the jet to resemble that of a w. When the jet vortices are drawn far away from the jet centerline because of the influence of the stronger wing vortices, the jet would only develop into the u shape seen in flow visualizations. For $\alpha = 25$ deg at three chords away, the jet vortices in the calculations are shown to be in the vicinity of the wing vortices but still not sufficiently close to be entrained by them. On the other hand, flow visualization showed the onset of jet effluent entrainment

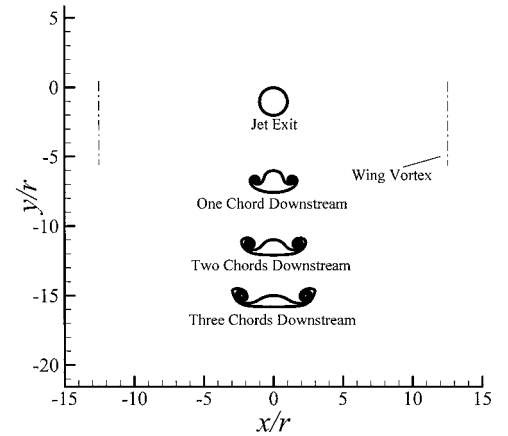

α = 5 deg

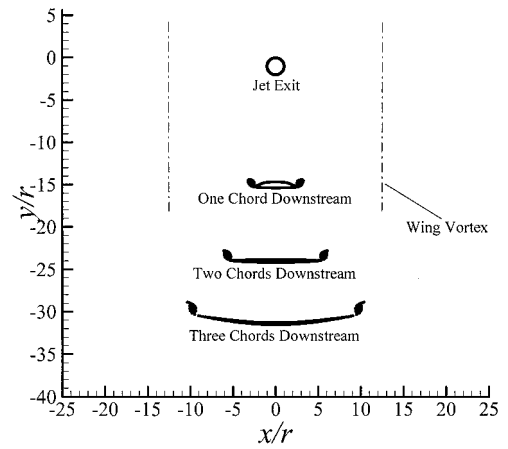

α = 15 deg

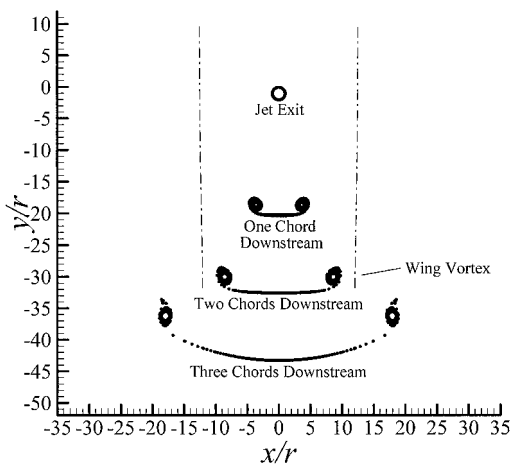

α = 25 deg

Fig. 10 Calculated jet development at three angles of attack and at three downstream locations.

into wing vortices in the case of $\alpha = 25$ deg and three chords away (Fig. 2). Instead, the calculation suggests the ingestion of the jet into wing vortices, indicated by the trajectories of wing and jet vortices intercepting each other, occurs later at approximately five chords downstream. The aforementioned phenomenon is illustrated in Fig. 11. Several reasons can contribute to this overprediction of the distance at which the effluent of the jet starts to be entrained into the wing vortices. Unlike vortices produced by lifting planforms, those generated by a jet in a crossflow are more diffuse and would have a comparatively rapid decay. Prescribing a constant strength for the jet vortices manifests itself in their traveling a longer distance downstream before being entrained by the wing vortices. In addition, the formulation does not account for the natural spreading of the jet, which again makes the present prediction more conservative. However, if the calculations were modified to perform a supersonic freestream case (i.e., by prescribing a different circulation information for the wing vortices), the results would be expected to be less conservative as the natural spreading of a supersonic jet is small.[29]

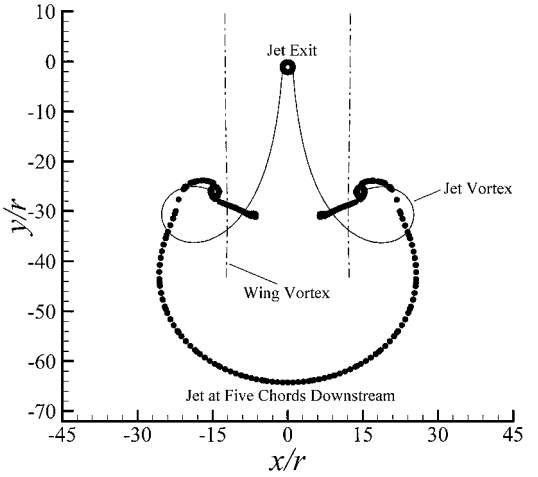

Fig. 11 Trajectories of jet and wing vortices for α = 25 deg and five chords downstream.

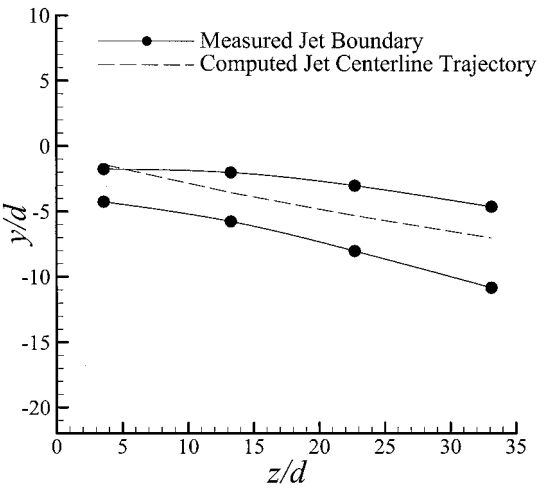

Fig. 12 Centerline trajectory of the jet at α = 15 deg.

The descending character of the jet observed in flow visualization is assessed with the aid of the modeling. For the particular case of $\alpha = 15$ deg where the descent of the jet is quantified, Fig. 12 shows the upper and lower jet boundaries as discerned by the total-pressure surveys superimposed on the calculated jet centerline trajectory. The jet boundary as disclosed by total pressure has a mild concave-down curvature within the first chord distance surveyed. Except for the few orifice diameters initially, satisfactory agreement is found between the trajectory suggested by the vortex-filament model and that of experiments. It suggests that the initial jet momentum is sufficient not to have been dominated by the descending vortex wake in the first few jet diameters, thereby manifesting itself in a trajectory trend different from that of the vortex wake and thus the development of the jet vortices. As enhanced lateral spreading of the jet occurs, axial velocity of the jet rapidly declines so that the subsequent evolution of the jet effluent would subsequently be determined by the persistent vortex-wake flow of the planform as per the suggestion of the experiments.

Conclusions

An experimental investigation of the near-field vortex-wake/jet interaction at low speed has been presented. The study used

flow-visualization, total-pressure measurements, and interpretation of the results was aided by a vortex-filament model. For the particular experimental configuration examined the data showed that the wing vortices were only mildly affected in terms of their trajectory by the jet, but the jet was significantly influenced by the presence of the wing vortices. Except for the first few orifice diameters downstream, the jet was dominated by the induced velocity field in the planform's vortex wake, and its subsequent development followed that of the convecting vortex wake of the planform. The existence of vortices developed from the jet being immersed in the vortex wake was verified through flow visualization. As the jet/vortex-wake interaction proceeded downstream, the cross-sectional shape of the jet in the current case can either be in the form of a w or a u, depending on the location of these jet vortices relative to the plane of symmetry. For a low angle-of-attack situation typical of aircraft at cruise, the jet vortices can remain longer in close vicinity of the symmetry plane and therefore can make a more significant contribution to the overall mixing and dispersion characteristics of exhaust products during the life span of the vortex wake. For moderate and high angles-of-attack cases, the jet vortices were quickly moved far from the plane of symmetry under the induced action of the strong wing vortices. In all cases the jet was compressed vertically but substantially elongated laterally. The horizontal spreading of the jet progressed nonlinearly with angles of attack. The merit of introducing well-organized and persistent streamwise vortices to increase the spread of a jet is therefore illustrated. Moreover, large spreading of the jet can be achieved at moderate angles of attack and within a short distance of three root chords downstream. The total pressure data revealed that the jet in a downwash field has a reduced potential core length and an accelerated maximum velocity decay compared to the parallel coflowing jet counterpart.

A vortex-filament model for examining aspects of the interaction between jets and planform vortices has been presented. The utilization of the model has been illustrated for a delta-wing/circular-jet configuration at low speed, and the manner in which results can be interpreted has been proposed. Comparisons with flow-visualization results indicated that the downstream distance for which the jet would start to be at least partially ingested by the wing vortices, as predicted on the basis of the model, would likely be conservative. The simplicity of the modeling approach and the reasonable qualitative results obtained make it attractive as a tool for planning additional experiments of this type in the future. For example, useful insights can be obtained regarding the sensitivities of various parameters for either promoting or delaying vortex ingestion of jet plumes, as well as devising strategies for augmented jet spreading in various technological areas. For instance, the model suggests that if additional strong and persistent vortices can be generated around the jet (e.g., by using tabs or fins), jet spreading beyond the span of the wing planform is attainable.

Acknowledgments

The support from the technical staff of the von Kármán Institute Aeronautics/Aerospace Department, Roger Conniasselle, Robert Voets, Philippe Salmon, and Patrick Danneels, is acknowledged with appreciation. Special thanks go to the National Science Foundation-NATO Postdoctoral Fellowship Program in Science and Engineering (Grant DGE-9633933) for providing financial support for the first author. The work was carried out in partial fulfillment for the Diploma Course program of the second author.

References

[1]Overcamp, T. J., and Fay, J. A., "Dispersion and Subsidence of the Exhaust of a Supersonic Transport in the Stratosphere," *Journal of Aircraft*, Vol. 10, No. 12, 1973, pp. 720–728.

[2]Nielsen, J. N., Stahar, S. S., and Woolley, J. P., "Ingestion and Dispersion of Engine Exhaust Products by Trailing Vortices for Supersonic Flight in the Stratosphere," AIAA Paper 74-42, Jan. 1974.

[3]Quackenbush, T. R., Teske, M. E., and Bilanin, A. J., "Dynamics of Exhaust Plume Entrainment in Aircraft Vortex Wakes," AIAA Paper 96-0747, Jan. 1996.

[4]Cali, P., and Drela, M., "Implicit Euler Calculation of Supersonic Vortex Wake/Engine Plume Interaction," AIAA Paper 93-0656, Jan. 1993.

[5]Miake-Lye, R. C., Martinez-Sanchez, M., Brown, R. C., and Kolb, C. E., "Plume and Wake Dynamics, Mixing, and Chemistry Behind a High Speed Civil Transport Aircraft," *Journal of Aircraft*, Vol. 30, No. 4, 1993, pp. 467–479.

[6]Poppoff, I. G., Farlow, N. H., and Anderson, L. B., "Studies of Aircraft Wake Chemistry and Dispersion," *Acta Astronautica*, Vol. 1, Jan.–Feb. 1974, pp. 157–178.

[7]Garnier, F., Baudoin, C., Woods, P., and Louisnard, N., "Engine Emission Alteration in the Near Field of An Aircraft," *Atmospheric Environment*, Vol. 31, No. 12, 1997, pp. 1767–1781.

[8]Gerz, T., and Ehret, T., "Wingtip Vortices and Exhaust Jets During the Jet Regime of Aircraft Wakes," *Aerospace Science and Technology*, Vol. 1, No. 7, 1997, pp. 463–474.

[9]Jacquin, L., and Garnier, F., "On the Dynamics of Engine Jets Behind a Transport Aircraft," *The Characterisation and Modification of Wakes from Lifting Vehicles in Fluids*, AGARD-CP-584, AGARD, Trondheim, Norway, 1996, pp. 37.1–37.8.

[10]Kandil, O. A., Adam, I., and Wong, T.-C., "Far-Field Turbulent Vortex-Wake/Exhaust Plume Interaction for Subsonic and HSCT Airplanes," AIAA Paper 96-1962, June 1996.

[11]Wu, J., and Menon, S., "Numerical Studies of Near-Field Plume Vortex Interaction," AIAA Paper 98-2902, June 1998.

[12]McCroskey, W. J., "Technical Evaluation Report—The Characterisation and Modification of Wakes from Lifting Vehicles in Fluids," AGARD-CP-584, Trondheim, Norway, 1996, pp. T1–T10.

[13]Zaman, K. B. M. Q., Reeder, M. F., and Samimy, M., "Control of an Axisymmetric Jet Using Vortex Generators," *Physics of Fluids*, Vol. 6, No. 2, Pt. 2, 1994, pp. 778–793.

[14]Dash, S. M., and Kenzakowski, D. C., "Turbulent Aspects of Plume Aerodynamic Interactions," AIAA Paper 95-2373, July 1995.

[15]Seiner, J. M., and Grosch, C. E., "Mixing Enhancement by Tabs in Round Supersonic Jets," AIAA Paper 98-2326, June 1988.

[16]Proot, M. M. J., Wang, F. Y., Sforza, P. M., and Charbonnier, J.-M., "Near-Field Vortex-Wake/Plume Interaction at Low Speed," *Proceedings of 1998 ASME Fluids Engineering Division Summer Meeting*, American Society of Mechanical Engineers Paper FEDSM98-4991, New York, 1998.

[17]Wang, F. Y., Proot, M. M. J., Charbonnier, J.-M., and Sforza, P. M., "Interaction of a Jet with Leading Edge Vortices," *Proceedings of 8th International Symposium on Flow Visualization*, Sorrento, Italy, 1998.

[18]El-Ramly, Z., and Rainbird, W. J., "Effect of Simulated Jet Engines on the Flowfield Behind a Swept-Back Wing," *Journal of Aircraft*, Vol. 14, No. 4, 1977, pp. 343–349.

[19]Abramovich, G. N., *The Theory of Turbulent Jets*, Massachusetts Inst. of Technology Press, Cambridge, MA, 1963, p. 201.

[20]Leonard, A., "Vortex Methods for Flow Simulation," *Journal of Computational Physics*, Vol. 37, 1980, pp. 289–335.

[21]Rossow, V. J., "Extended-Betz Methods for Roll-Up of Vortex Sheets," *Journal of Aircraft*, Vol. 34, No. 5, 1997, pp. 592–599.

[22]Fearn, R. L., and Weston, R. P., "Velocity Field of a Round Jet in a Cross Flow for Various Jet Injection Angles and Velocity Ratios," NASA TP 1506, Oct. 1979.

[23]Sforza, P. M., "Interaction of Wing Vortices and Plumes in Supersonic Flight," *Proceedings of the International Union of Theoretical and Applied Mechanics Symposium on Dynamics of Slender Vortices*, Kluwer Academic, Norwell, MA, 1998, pp. 415–424.

[24]Kimball, D. F., "Laser Doppler Velocity Measurements in the Primary Vortices Above a Slender Delta Wing at High Angles of Attack," von Kármán Inst., Project Rept. 1984-03, Sint-Genesius-Rode, Belgium, June 1984.

[25]Hemsch, M. J., and Luckring, J. M., "Connection Between Leading-Edge Sweep, Vortex Lift, and Vortex Strength for Delta Wing," *Journal of Aircraft*, Vol. 27, No. 5, 1990, pp. 473–475.

[26]Traub, L. W., "Prediction of Delta Wing Leading-Edge Vortex Circulation and Lift-Curve Slope," *Journal of Aircraft*, Vol. 34, No. 3, 1997, pp. 450–452.

[27]Anderson, J. D., Jr., *Fundamentals of Aerodynamics*, 2nd ed., McGraw–Hill, New York, 1991, pp. 320–324.

[28]Spalart, P. R., "Vortex Methods for Separated Flows," VKI-LS 1988-05: *Computational Fluid Dynamics Lecture Series*, von Kármán Inst. for Fluid Dynamics, Sint-Genesius-Rode, Belgium, 1988.

[29]Wilder, J. G., Jr., and Hindersinn, K., "Spreading of Supersonic Jets in Supersonic Streams," *Aeronautical Engineering Review*, Oct. 1953, pp. 54–68.